



# Magnetic resonance imaging improves stratification of fibrosis and steatosis in patients with chronic liver disease

Han Ah Lee<sup>1</sup> · Seung-seob Kim<sup>2</sup> · Jin-Young Choi<sup>2</sup> · Yeon Seok Seo<sup>3</sup> · Beom Jin Park<sup>4</sup> · Ki Choon Sim<sup>4</sup> · Seung Up Kim<sup>5,6</sup>

Received: 29 May 2022 / Revised: 11 July 2022 / Accepted: 11 July 2022 / Published online: 13 August 2022  
© The Author(s), under exclusive licence to Springer Science+Business Media, LLC, part of Springer Nature 2022

## Abstract

**Purpose** We aimed to compare the diagnostic accuracy of magnetic resonance imaging (MRI) and transient elastography (TE) in assessing liver fibrosis and steatosis in patients with chronic liver disease (CLD).

**Methods** Patients who underwent liver biopsy or liver surgery at two academic hospitals between 2017 and 2021 were retrospectively recruited. The stages of liver fibrosis and steatosis were evaluated using histologic examination. Liver stiffness (LS) was assessed using MR elastography ( $LS_{MRE}$ ) and TE ( $LS_{TE}$ ). Liver steatosis was assessed using proton density fat fraction (PDFF) and controlled attenuation parameter (CAP).

**Results** The mean age of the study population ( $n = 280$ ) was 53.6 years and male sex predominated ( $n = 199$ , 71.1%). Non-alcoholic fatty liver disease was the most prevalent ( $n = 127$ , 45.5%), followed by hepatitis B virus ( $n = 112$ , 40.0%). Hepatocellular carcinoma was identified in 130 patients (46.4%). The proportions of F0, F1, F2, F3, and F4 fibrosis were 13.2%, 31.1%, 9.6%, 16.4%, and 29.7%, respectively.  $LS_{MRE}$  had a significantly greater AUROC value than  $LS_{TE}$  for detecting F2–F4 (0.846 vs. 0.781,  $P = 0.046$ ), whereas  $LS_{MRE}$  and  $LS_{TE}$  similarly predicted F1–4, F3–4, and F4 (all  $P > 0.05$ ). The proportions of S0, S1, S2, and S3 steatosis were 34.7%, 49.6%, 12.5%, and 3.2%, respectively. PDFF had significantly greater AUROC

---

Han Ah Lee and Seung-seob Kim have equally contributed to this article as co-first authors.

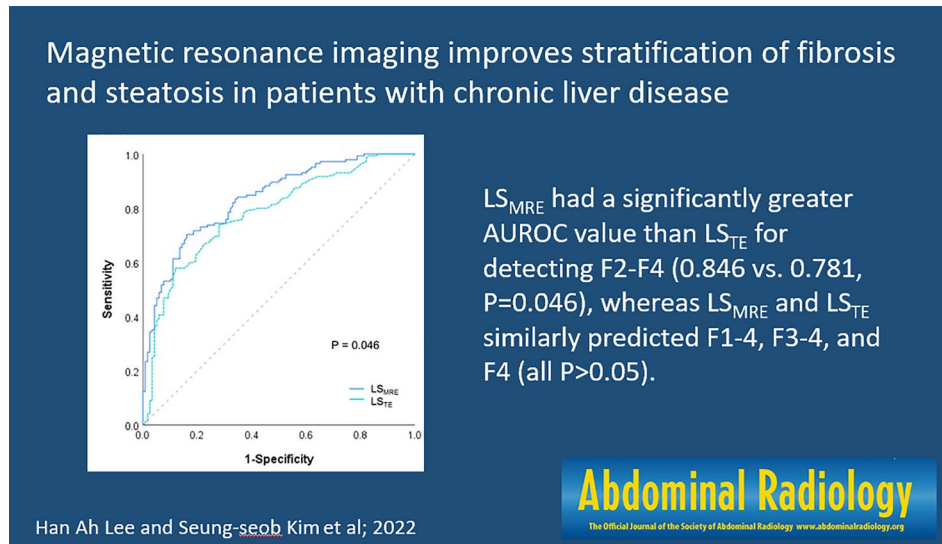
- 
- ✉ Jin-Young Choi  
gafield2@yuhs.ac
  - ✉ Ki Choon Sim  
ha2sky@hanmail.net
  - ✉ Seung Up Kim  
KSUKOREA@yuhs.ac

- <sup>1</sup> Department of Internal Medicine, College of Medicine, Ewha Womans University, Seoul, South Korea
- <sup>2</sup> Department of Radiology and Research Institute of Radiological Science, Severance Hospital, Yonsei University College of Medicine, 50-1 Yonsei-ro, Seodaemun-gu, Seoul 03722, Republic of Korea
- <sup>3</sup> Departments of Internal Medicine, Korea University College of Medicine, Seoul, South Korea
- <sup>4</sup> Department of Radiology, Korea University College of Medicine, 73, Goryeodae-ro, Seongbuk-gu, Seoul, South Korea
- <sup>5</sup> Department of Internal Medicine, Yonsei University College of Medicine, 50-1, Yonsei-ro, Seodaemun-gu, Seoul, South Korea
- <sup>6</sup> Yonsei Liver Center, Severance Hospital, Seoul, South Korea

values than CAP in predicting S1-3 (0.922 vs. 0.806,  $P < 0.001$ ) and S2-3 (0.924 vs. 0.795,  $P = 0.005$ ); however, PDFF and CAP similarly predicted S3 ( $P = 0.086$ ).

**Conclusion** MRI exhibited significantly higher diagnostic accuracy than TE for detecting significant fibrosis and mild or moderate steatosis in patients with CLD.

### Graphical abstract



$LS_{MRE}$  had a significantly greater AUROC value than  $LS_{TE}$  for detecting F2-F4 (0.846 vs. 0.781,  $P = 0.046$ ), whereas  $LS_{MRE}$  and  $LS_{TE}$  similarly predicted F1-4, F3-4, and F4 (all  $P > 0.05$ ).

**Keywords** MR elastography · Proton density fat fraction · Transient elastography · Controlled attenuation parameter · Histology

### Abbreviations

CLD	Chronic liver disease
HCC	Hepatocellular carcinoma
LS	Liver stiffness
TE	Transient elastography
MRE	Magnetic resonance elastography
CAP	Controlled attenuation parameter
NAFLD	Nonalcoholic fatty liver disease
PDFF	Proton density fat fraction
$LS_{MRE}$	Liver stiffness assessed using magnetic resonance elastography
$LS_{TE}$	Liver stiffness assessed using transient elastography
HCV	Hepatitis B and C virus
ROI	Region of interest
BMI	Body mass index
IQR	Interquartile range
PPV	Positive predictive value
NPV	Negative predictive value
AUROC	Areas under the receiver operating characteristic
CI	Confidence interval
ALT	Alanine aminotransferase

### Introduction

Liver fibrosis is one of the main prognostic factors in chronic liver disease (CLD) as there is an exponential increase in the risk of liver-related complications with increasing fibrosis stage [1–3]. In addition, recent studies reported that superimposed liver steatosis was associated with a higher risk of hepatocellular carcinoma (HCC) [4]. Therefore, quantifying liver fibrosis and steatosis in patients with CLD is important to determine the prognosis and guide treatment decisions.

Liver biopsy represents the gold standard for the assessment of fibrosis and steatosis in patients with CLD [5]. However, several issues, including invasiveness, patient discomfort, and risk of sampling error due to the heterogeneity in the distribution of fibrosis or steatosis, have been continuously raised [6–10]. Accordingly, several alternative non-invasive tests are increasingly being used to improve the stratification and prognostication of patients with CLD [11].

Vibration-controlled transient elastography (TE) is the most widely validated diagnostic method for the measurement of liver stiffness (LS). However, the LS value obtained by TE can overestimate the severity of fibrosis in cases, including inflammation or obstructive cholestasis [12–16]. Magnetic resonance elastography (MRE) is thought to be

more reliable than TE in the assessment of LS because it can examine the larger area of liver parenchyma using a magnetic resonance imaging (MRI) machine. Although several studies including meta-analysis suggested the superiority of MRE than TE for detecting significant or advanced fibrosis and cirrhosis, other study of 62 biopsy-proven NAFLD patients showed comparable diagnostic accuracy for significant and advanced fibrosis. [17–19].

The controlled attenuation parameter (CAP) implemented on TE enables rapid assessment of liver steatosis. However, the suboptimal performance of CAP for quantifying steatosis has been reported. Furthermore, in patients with nonalcoholic fatty liver disease (NAFLD), CAP has been reported to be outperformed by proton density fat fraction (PDFFF), a MRI-based method that quantitatively assesses liver steatosis [18, 20]. However, in CLD with various etiology, only small-sized studies comparing MRI and TE in assessing liver fibrosis and steatosis have been performed.

This study aimed at the comparison of the diagnostic accuracy of LS assessed using MRE ( $LS_{MRE}$ ) and TE ( $LS_{TE}$ ) for determining the degree of liver fibrosis and PDFFF and CAP for assessing liver steatosis in patients with CLD.

## Materials and methods

### Study population

This cross-sectional study included patients with CLD who had undergone a liver biopsy, surgical resection, or liver transplantation between August 2017 and March 2021 and were referred to the Korea University Anam Hospital

and Yonsei University Severance Hospital. Each subject underwent MRE, PDFFF, TE, and CAP, and the time interval between those and liver biopsy, surgical resection, or liver transplantation was < 6 months (Fig. 1). The exclusion criteria were as follows: (a) age < 18 years, (b) insufficient clinical or laboratory information, (c) history of decompensation, (d) obstructive cholestasis, (e) liver congestion, (f) acute hepatitis, and (g) infiltrative liver diseases.

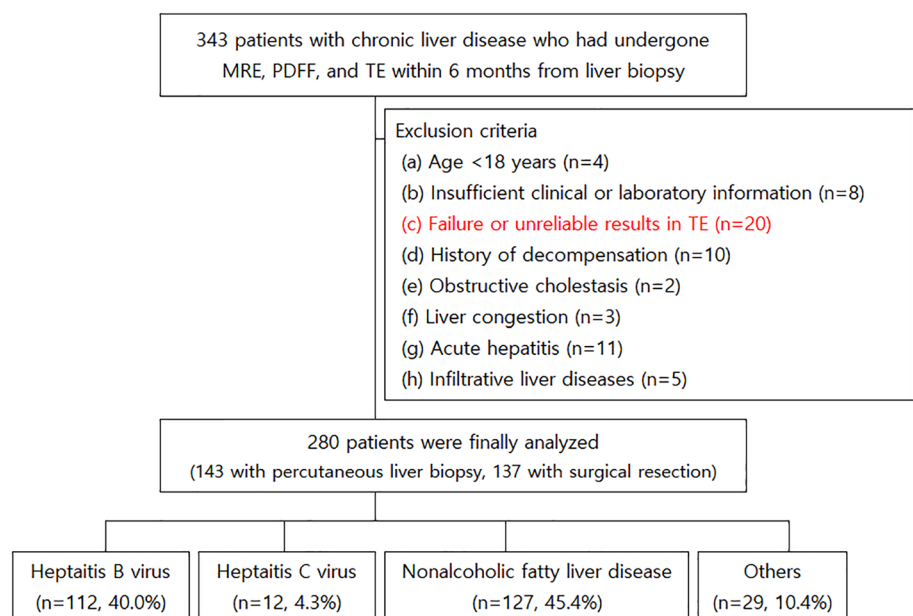
Hepatitis B and C virus (HCV) infection was defined as positive for hepatitis B surface antigen and anti-HCV, respectively. Diagnosis of NAFLD was established by the absence of significant alcohol intake (weekly consumption > 140 g for men or > 70 g for women), absence of other causes of CLD, and fat accumulation of more than 5% of the liver weight in liver biopsy specimens [21].

### Histopathological evaluation

Histopathological analysis was performed on specimens from percutaneous liver biopsy ( $n = 143$ ), surgical resection ( $n = 86$ ), or liver transplantation ( $n = 51$ ). Ultrasonography-guided liver biopsies were performed by expert radiologists or hepatologists experienced with more than 200 liver biopsies. A transthoracic approach was routinely used with the patient in the supine position. Biopsy was performed using an 18- or 20-gauge Tru-cut needle, and two specimens were obtained from each patient to acquire a sample of sufficient size for analysis and to reduce histologic errors.

Each liver tissue was analyzed by two experienced pathologists who were blinded to the patients' clinical information. The minimum adequacy of the specimen was defined as a length longer than 2 cm [8]. Liver fibrosis was

**Fig. 1** Flowchart of patients. *MRE* magnetic resonance elastography, *PDFFF* proton density fat fraction, *TE* transient elastography



staged according to the Nonalcoholic steatohepatitis Clinical Research Network scoring system in NAFLD and the METAVIR scoring system in other etiologies, ranging from F0 to F4 [6, 7]. Liver steatosis was graded on the basis of the percentage of hepatocytes with macrovesicular fat: S0 (none or less than 5%), S1 (mild steatosis = 6–33%), S2 (moderate steatosis = 34–66%), and S3 (severe steatosis = greater than 66%) [22].

### Magnetic resonance elastography

MRE examinations were performed using the 3.0-T scanner (Magnetom Skyra, Siemens Healthineers, Erlangen, Germany; Discovery 750w, GE Healthcare, Milwaukee, WI, USA). In the supine position, the passive acoustic driver was placed on the right upper abdominal wall, with its center at the level of the xiphoid process. Driver power amplitude of 50% was used for each patient during the study period. MRE was performed using a phase-contrast imaging technique, which applies motion-encoding gradients in synchronization with a 60-Hz external shear wave induced in the abdomen. Four contiguous slices were obtained during breath-hold at the end of expiration. After the magnitude and phase images were obtained, an inversion algorithm installed in the MRI unit automatically processed raw data images to create the wave images and the elastograms with confidence maps of a 95% confidence threshold.

A radiologist with 10 years of experience in abdominal radiology drew three or four freehand areas of the region of interest (ROI), carefully avoiding the following areas: cross-hatched areas on the superimposed 95% confidence map, areas of poor wave propagation or wave distortion, liver dome, large blood vessels, and focal hepatic mass.  $LS_{MRE}$  is calculated using the following equation:  $LS_{MRE} = (m_1w_1 + m_2w_2 + m_3w_3 + m_4w_4)/(w_1 + w_2 + w_3 + w_4)$ , where  $m_1$ ,  $m_2$ ,  $m_3$ , and  $m_4$  are the mean LS values measured on up to four elastograms, and  $w_1$ ,  $w_2$ ,  $w_3$ , and  $w_4$  are the

sizes of the corresponding ROIs [23]. Detailed parameters for MRE are described in Table 1.

### Magnetic resonance imaging-based proton density fat fraction

PDFF examinations were performed during a single breath-hold, using commercially available chemical shift-encoded pulse sequences of q-DIXON (Siemens Healthineers, Erlangen, Germany) or IDEAL IQ (GE Healthcare, Milwaukee, WI, USA). A radiologist with 10 years of experience in abdominal radiology drew four oval ROIs ( $\geq 4 \text{ cm}^2$ ) in each of the right anterior, right posterior, left medial, and left lateral segments of the liver, carefully avoiding large blood vessels and focal hepatic mass. For the measurement of steatosis using PDFF, the mean values of the four ROIs were calculated for statistical analysis [24]. Detailed parameters for PDFF are described in Table 1.

### Transient elastography

At each hospital, the  $LS_{TE}$  was obtained using TE (M-probe, Fibrosan: EchoSens, Paris, France) by an experienced operator who had conducted at least 500 examinations. Patients were examined after overnight fasting using M probes, considering the patients' body mass index.  $LS_{TE}$  (kPa) and CAP (dB/m) measurements were recorded until 10 valid measurements were obtained for each patient. The median value was considered representative of the elastic modulus of the liver. Only procedures with at least 10 valid measurements, a success rate of at least 60%, and an interquartile range (IQR) to median value ratio of 30% were considered reliable [11, 25].

### Statistical analysis

Demographic and laboratory data were presented as mean  $\pm$  standard deviation for continuous variables and numbers with percentages for categorical variables. The

**Table 1** Detailed parameters for magnetic resonance elastography and proton density fat fraction

Vendor/parameters	Elastography		Proton density fat fraction	
Vendor	Magnetom Skyra, Siemens	Discovery 750w, GE	Magnetom Skyra, Siemens	Discovery 750w, GE
Pulse sequence	2D gradient-recalled echo	2D spin-echo Echo-planar imaging	q-DIXON	IDEAL IQ
Field of view (mm)	420 × 295	380 × 380	380 × 304	400 × 320
Repetition time (msec)	25	1000	9	7.2
Echo time (msec)	17–20	63	1	3
Acquisition matrix	128 × 63	64 × 64	160 × 115	160 × 128
Slice thickness (mm)	5	8	3	6
Flip angle (°)	25	90	4	4

distribution of mean LS and steatosis values in each fibrosis and steatosis group were compared using Kruskal–Wallis test and trend test was performed. Trend test was conducted using linear regression analysis with severity of liver fibrosis or liver steatosis applied as an ordinal value. Sensitivity, specificity, positive predictive value (PPV), and negative predictive value (NPV) at optimal cutoff values for estimating fibrosis and steatosis were evaluated. The optimal cutoff values were chosen by maximizing the Youden index on the estimated curves (sensitivity + specificity - 1). For the discrimination ability of mean LS and steatosis values, the areas under the receiver operating characteristic (AUROC) curves and 95% confidence intervals (95% CI) were estimated. The standard error of AUROC was estimated under nonparametric assumption and asymptotic confidence interval was presented. The AUROC values of each assessment were compared using the DeLong test [26]. We performed fivefold cross-validation to avoid potential bias. The 95% CI was estimated based on the normal distribution theory. Post hoc power analysis was performed to verify the soundness of the accurate comparison using the pROC package of R software. Regression analyses of the clinical and histopathological characteristics of patients were performed to identify predictors associated with  $LS_{MRE}$  and  $LS_{TE}$ . A two-tailed  $P$  value  $< 0.05$  was considered statistically significant. Statistical analyses were performed using SPSS software (version 25.0; International Business Machines Corp.) and R software (version 3.6.1; R Foundation for Statistical Computing, Vienna, Austria).

## Results

### Patient characteristics

Among the 343 patients who were considered eligible, 42 were excluded according to our exclusion criteria. Finally, 280 patients were selected for the statistical analysis. Histopathological evaluation was performed through liver biopsy in 143 patients, surgical resection in 86 patients, and liver transplantation in 51 patients. The median time interval between imaging examinations and pathological results was 0.8 (interquartile range, 0.2–3.2) months. Table 2 details the features and characteristics of the enrolled patients.

The mean age was 53.6 years and the male sex was predominant (199 patients, 71.1%). NAFLD was the most prevalent etiology (127 patients, 45.5%), followed by hepatitis B virus (112 patients, 40.0%). HCC was present in 130 patients (46.4%). The mean platelet count and alanine aminotransferase (ALT) level were  $184.3 \times 10^9/L$  and 92.8 IU/L, respectively. The proportions of patients in each fibrosis stage were 13.2% ( $n = 37$ ), 31.1% ( $n = 87$ ), 9.6% ( $n = 27$ ), 16.4% ( $n = 46$ ), and 29.7% ( $n = 83$ ) in stages 0, 1, 2, 3, and 4,

**Table 2** Baseline characteristics of patient population ( $n = 280$ )

Variables	Values
Demographic variables	
Age, years	53.6 ± 20.3
Male	199 (71.1)
Etiology	
Hepatitis B virus	112 (40.0)
Hepatitis C virus	12 (4.3)
Nonalcoholic fatty liver	127 (45.4)
Alcohol	7 (2.5)
Others	22 (7.9)
Hypertension	120 (42.9)
Diabetes	94 (34.1)
Body mass index	26.4 ± 21.4
Hepatocellular carcinoma	130 (46.4)
Laboratory variables	
Hemoglobin, g/dL	13.2 ± 2.4
Platelet count, $\times 10^9/L$	184.3 ± 80.0
Serum creatinine, mg/dL	0.8 ± 0.2
INR	1.1 ± 0.3
Aspartate aminotransferase, IU/L	90.7 ± 79.2
Alanine aminotransferase, IU/L	92.8 ± 84.0
Total bilirubin, mg/dL	1.3 ± 1.0
Serum albumin, g/dL	3.9 ± 0.6
Triglyceride, mg/dL	139.6 ± 111.3
Total cholesterol, mg/dL	148.8 ± 55.3
Fibrosis stage	
F0/F1/F2/F3/F4	37 (13.2)/87 (31.1)/27 (9.6)/46 (16.4)/83 (29.7)
Steatosis grade	
S0/S1/S2/S3	97 (34.7)/139 (49.6)/35 (12.5)/9 (3.2)

Variables are expressed as mean ± standard deviation or n (%)

INR international normalized ratio

respectively. When patients were classified according to the grade of hepatic steatosis, 34.7% ( $n = 97$ ), 49.6% ( $n = 139$ ), 12.5% ( $n = 35$ ), and 3.2% ( $n = 9$ ) of patients had grade 0, 1, 2, and 3 steatosis, respectively.

### Assessment of liver fibrosis

The  $LS_{MRE}$  and  $LS_{TE}$  were measured to assess the diagnostic accuracy for the stratification of the liver fibrosis stage. The mean  $LS_{MRE}$  for fibrosis stages 0, 1, 2, 3, and 4 were 2.5, 2.7, 3.3, 3.4, and 5.4 kPa, respectively (Kruskal–Wallis test  $P < 0.001$ ). The mean  $LS_{TE}$  ( $n = 263$ ) for fibrosis stages 0, 1, 2, 3, and 4, were 8.5, 8.8, 9.0, 12.5, and 19.9 kPa,



respectively (Kruskal–Wallis test  $P < 0.001$ ). We found stepwise increases in the  $LS_{MRE}$  and  $LS_{TE}$  with increasing histologic severity of liver fibrosis (all  $P < 0.001$  using the trend test) (Fig. 2).

### AUROC values of LSMRE and LSTE in in staging liver fibrosis

The AUROC values of  $LS_{MRE}$  and  $LS_{TE}$  in staging liver fibrosis are presented in Table 3. The AUROC values of  $LS_{MRE}$  for differentiating between stage F0 vs. F1–4, F0–1 vs. F2–4, F0–2 vs. F3–4, and F0–3 vs. F4 were 0.734 (95% CI 0.640–0.829), 0.846 (95% CI 0.801–0.890), 0.841 (95% CI 0.796–0.887), and 0.904 (95% CI 0.868–0.939), respectively. Corresponding values of  $LS_{TE}$  were 0.680 (95% CI 0.574–0.787), 0.781 (95% CI 0.714–0.829), 0.807 (95% CI 0.745–0.855), and 0.852 (95% CI 0.803–0.901), respectively.

### Comparison of diagnostic accuracies for staging liver fibrosis between LSMRE and LSTE

$LS_{MRE}$  had a significantly greater AUROC value than  $LS_{TE}$  for detecting METAVIR stages F2–F4 (0.846 vs. 0.781,  $P = 0.046$ , post hoc statistical power = 0.81). In fivefold cross-validation analysis, the AUROC value of  $LS_{MRE}$  was greater than that of  $LS_{TE}$  for detecting F2–F4 (0.761 vs. 0.712). Moreover,  $LS_{MRE}$  and  $LS_{TE}$  similarly predicted the F1–4 stage (AUROC = 0.734 vs. 0.680,  $P = 0.457$ ), F3–4 stage (AUROC = 0.841 vs. 0.807,  $P = 0.259$ ), and F4 stage fibrosis (AUROC = 0.904 vs. 0.852,  $P = 0.093$ ) (Fig. 3).

### Cutoff values of LSMRE and LSTE for staging liver fibrosis

The potential cutoff values of  $LS_{MRE}$  and  $LS_{TE}$  for the detection of each liver fibrosis stage were evaluated. The

cutoff values of  $LS_{MRE}$  for differentiating between stage F0 vs. F1–4, F0–1 vs. F2–4, F0–2 vs. F3–4, and F0–3 vs. F4 were 2.4, 3.1, 3.2, and 3.4 kPa, respectively. The corresponding values of  $LS_{TE}$  were 6.5, 11.2, 11.5, and 11.7 kPa, respectively.

Using a cutoff value of 3.1 kPa,  $LS_{MRE}$  had a sensitivity of 71.8%, specificity of 83.9%, positive predictive value (PPV) of 84.8%, and negative predictive value (NPV) of 70.3% for detecting significant fibrosis (F2–4).  $LS_{TE}$  of 11.2 kPa predicted significant fibrosis with a sensitivity of 57.9%, specificity of 88.1%, PPV of 85.7%, and NPV of 63.0%.

For the prediction of F4 fibrosis,  $LS_{MRE}$  had a sensitivity of 85.5%, specificity of 79.7%, PPV of 64.0%, and NPV of 92.9% with a cutoff value of 3.4 kPa. Using a cutoff value of 11.7 kPa,  $LS_{TE}$  showed a sensitivity of 81.1%, specificity of 82.5%, PPV of 64.5%, and NPV of 91.8% for detecting cirrhosis. The representative images of MRE and TE are presented in Fig. 4.

### Effects of clinical and histopathological characteristics on LSMRE and LSTE

The results of regression analysis for predictors associated with  $LS_{MRE}$  and  $LS_{TE}$  are presented in Table 4. In multivariate analysis, liver fibrosis was the only significant predictor of  $LS_{MRE}$  ( $\beta = 2.679$ , 95% CI 1.536–3.823,  $P < 0.001$ ) and  $LS_{TE}$  ( $\beta = 2.613$ , 95% CI 1.508–3.718,  $P < 0.001$ ).

### Assessment of steatosis

Fat accumulation obtained using PDFF and CAP was compared with the steatosis grade obtained by liver histology. The mean proportions of steatosis obtained using PDFF were 2.4%, 10.6%, 22.7%, and 34.8% for S0, 1, 2, and 3, respectively (Kruskal–Wallis test  $P < 0.001$ ). The mean

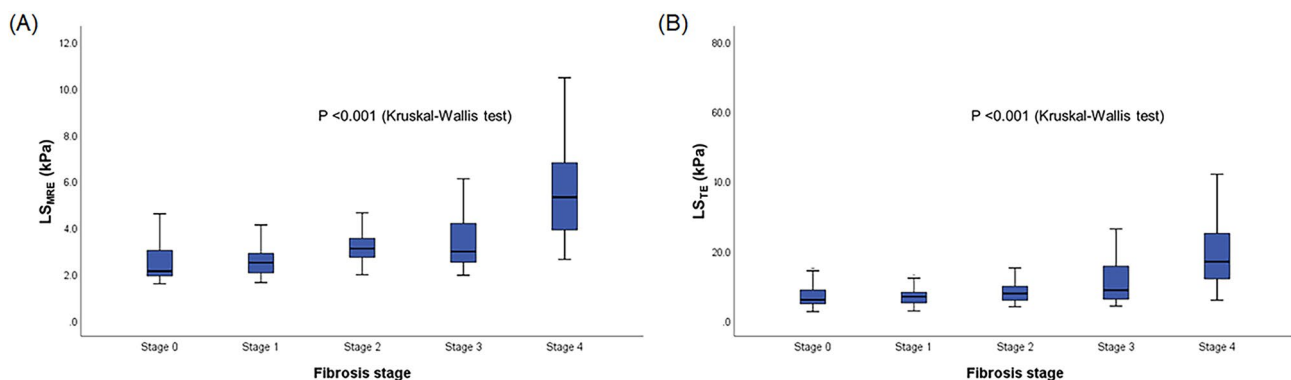


**Fig. 2** The mean  $LS_{MRE}$  (A) and  $LS_{TE}$  (B) according to each METAVIR fibrosis stage (F0 to F4). The horizontal line through each box represents the median and each box represents data from the 25th to

the 75th percentile. The separate asterisks and circles represent outliers.  $LS_{MRE}$  liver stiffness assessed using magnetic resonance elastography,  $LS_{TE}$  liver stiffness assessed using transient elastography

**Table 3** Diagnostic accuracy of  $L_{SMRE}$ ,  $L_{STE}$ , MR-PDFF, and CAP in each stage of fibrosis and steatosis

Category	Stage	AUROC (95% CI)	Cutoff	Sensitivity (%)	Specificity (%)	PPV (%)	NPV (%)	P value	vs. MR P value	AUROC from the fivefold cross-validation (95% CI)
$L_{SMRE}$	F0 vs. F1–4	0.734 (0.640–0.829)	2.4 kPa	80.7	64.9	93.8	33.8	<0.001	–	0.868 (0.851–0.885)
	F0–1 vs. F2–4	0.846 (0.801–0.890)	3.1 kPa	71.8	83.9	84.8	70.3	<0.001	–	0.761 (0.624–0.898)
	F0–2 vs. F3–4	0.841 (0.796–0.887)	3.2 kPa	69.8	85.4	80.4	76.8	<0.001	–	0.764 (0.697–0.832)
	F0–3 vs. F4	0.904 (0.868–0.939)	3.4 kPa	85.5	79.7	64.0	92.9	<0.001	–	0.829 (0.766–0.892)
	F0 vs. F1–4	0.680 (0.574–0.787)	6.5 kPa	71.5	65.7	93.1	26.1	<0.001	0.457	0.876 (0.857–0.894)
$L_{STE}$	F0–1 vs. F2–4	0.781 (0.714–0.829)	11.2 kPa	57.9	88.1	85.7	63.0	<0.001	0.046	0.712 (0.621–0.804)
	F0–2 vs. F3–4	0.807 (0.745–0.855)	11.5 kPa	66.1	86.9	80.4	75.9	<0.001	0.259	0.728 (0.603–0.853)
	F0–3 vs. F4	0.857 (0.803–0.901)	11.7 kPa	81.1	82.5	64.5	91.8	<0.001	0.093	0.774 (0.699–0.850)
PDFF	S0 vs. S1–3	0.922 (0.889–0.956)	4.2%	85.7	87.6	93.2	75.7	<0.001	–	0.852 (0.810–0.895)
	S0–1 vs. S2–3	0.924 (0.876–0.973)	11.9%	97.7	76.8	45.7	99.4	<0.001	–	0.906 (0.815–0.996)
	S0–2 vs. S3	0.958 (0.917–0.998)	18.9%	100.0	83.5	17.6	100.0	<0.001	–	0.970 (0.928–1.000)
CAP	S0 vs. S1–3	0.806 (0.750–0.863)	256 dB/m	82.0	69.7	83.0	68.1	<0.001	<0.001	0.760 (0.630–0.890)
	S0–1 vs. S2–3	0.795 (0.719–0.871)	294 dB/m	84.2	71.2	34.4	96.2	<0.001	0.005	0.840 (0.767–0.913)
	S0–2 vs. S3	0.760 (0.538–0.981)	294 dB/m	87.5	64.5	7.5	99.4	<0.001	0.086	0.968 (0.948–0.989)

$L_{SMRE}$  liver stiffness assessed using magnetic resonance elastography,  $L_{STE}$  liver stiffness assessed using transient elastography, PDFF proton density fat fraction, CAP controlled attenuation parameter, AUROC areas under the receiver operating characteristic, CI confidence interval, PPV positive predictive value, NPV negative predictive value

**Fig. 3** The area under the receiver operating characteristic curve of  $LS_{MRE}$  and  $LS_{TE}$  for staging liver fibrosis; F1–4 (A), F2–4 (B), F3–4 (C), and F4 (D).  $LS_{MRE}$  liver stiffness assessed using magnetic resonance elastography,  $LS_{TE}$  liver stiffness assessed using transient elastography

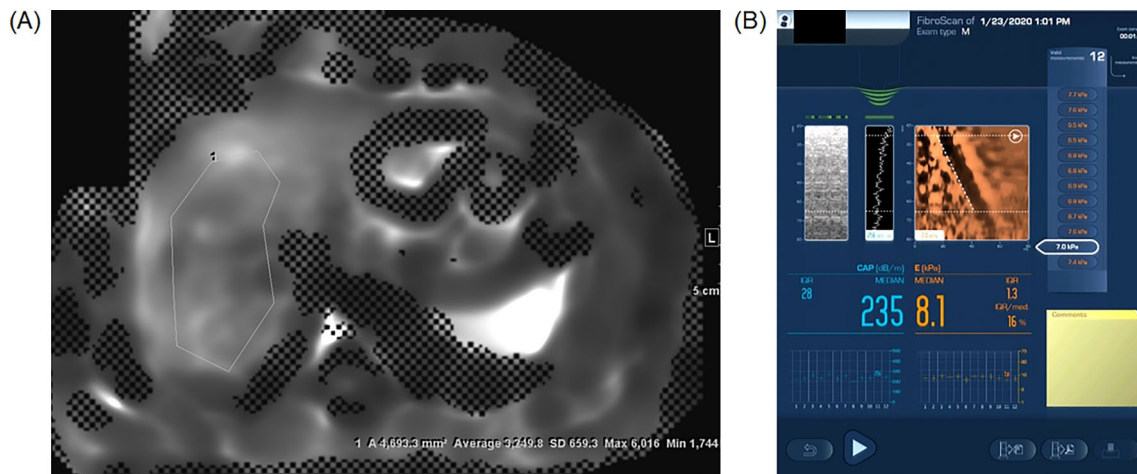
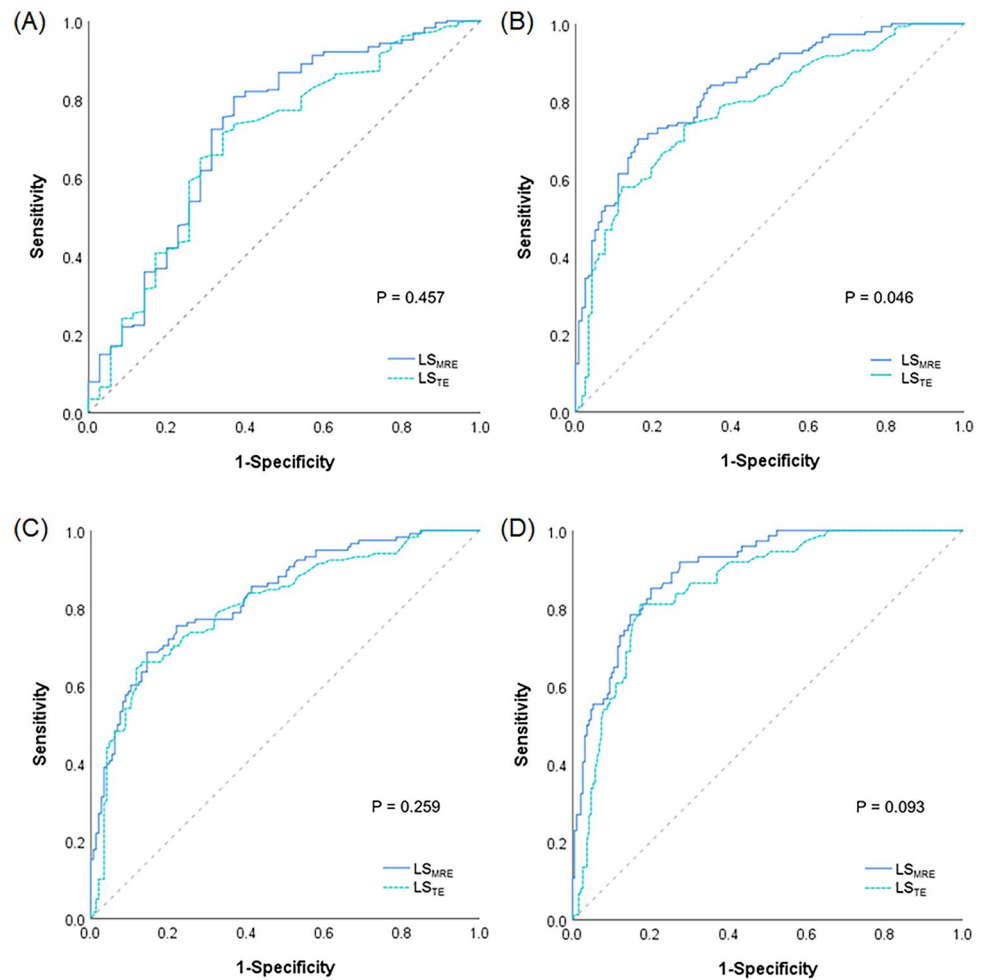


**Fig. 4** A 48-year-old male patient with newly diagnosed hepatocellular carcinoma underwent MRE and TE. **A** Representative image of MRE is shown with the freehand ROI drawn on the liver. The area of the ROI and the measured mean stiffness are  $4693 \text{ mm}^2$  and  $3.2 \text{ kPa}$ , respectively. Final liver stiffness was calculated as  $3.1 \text{ kPa}$  by the equation integrating the total of four MRE measurements. Using a

cutoff value of  $3.1 \text{ kPa}$ , liver fibrosis stage of F2–4 was suggested. **B** Summary of TE measurement is shown with the final liver stiffness of  $8.1 \text{ kPa}$ , which suggests liver fibrosis stage of F1–4 based on a cutoff value of  $6.5 \text{ kPa}$ . Liver resection was performed, and the histopathologic grade of liver fibrosis was F2. *MRE* magnetic resonance elastography, *TE* transient elastography, *ROI* region of interest



**Table 4** Predictors for  $LS_{MRE}$  and  $LS_{TE}$

Variables	Rating	$LS_{MRE}$				$LS_{TE}$			
		Univariate		Multivariate		Univariate		Multivariate	
		$\beta$ (95% CI)	<i>P</i> value	$\beta$ (95% CI)	<i>P</i> value	$\beta$ (95% CI)	<i>P</i> value	$\beta$ (95% CI)	<i>P</i> value
Age	Years	0.044 (0.030 to 0.058)	<0.001	0.008 (− 0.007–0.022)	0.284	0.165 (0.069 to 0.261)	0.002	0.007 (− 0.104–0.117)	0.903
Sex	0 = women; 1 = men	0.386 (− 0.083 to 0.106 0.855)				1.627 (− 1.385 to 0.273 4.639)			
Body mass index	kg/m <sup>2</sup>	− 0.086 (− 0.131 to − 0.041)	<0.001	0.022 (− 0.022–0.067)	0.324	− 0.373 (− 0.682 to − 0.064)	0.014	0.051 (− 0.305–0.406)	0.778
Aspartate aminotransferase	IU/L	0.007 (0.005 to 0.010)	<0.001	0.001 (− 0.002–0.004)	0.390	0.040 (0.023 to 0.057)	<0.001	0.019 (− 0.005–0.042)	0.122
Alanine aminotransferase	IU/L	0.003 (0.001 to 0.006)	0.013	0.001 (− 0.001–0.004)	0.269	0.022 (0.005 to 0.038)	0.008	0.006 (− 0.016–0.027)	0.596
Fibrosis	F0–F4	0.754 (0.639 to 0.869)	<0.001	2.679 (1.536–3.823)	<0.001	3.092 (2.219 to 3.964)	<0.001	2.613 (1.508–3.718)	<0.001
Steatosis	S0–S3	− 0.664 (− 0.934 to − 0.393)	<0.001	− 0.151 (− 0.416–0.115)	0.264	− 2.548 (− 4.325 to − 0.770)	0.008	− 0.322 (− 2.340–1.696)	0.754

$LS_{MRE}$  liver stiffness assessed using magnetic resonance elastography,  $LS_{TE}$  liver stiffness assessed using transient elastography, *CI* confidence interval

CAP values were 240.1 dB/m, 288.6 dB/m, 323.7 dB/m, and 326.4 dB/m for S0, 1, 2, and 3, respectively (Kruskal–Wallis test  $P < 0.001$ ). Stepwise increases in the steatosis values obtained using PDFF and CAP with increasing histologic severity of liver steatosis were found (all  $P < 0.001$  using the trend test) (Fig. 5).

**The AUROC values of PDFF and CAP in staging liver steatosis**

The AUROC values of PDFF and CAP for differentiating between each liver steatosis grade are presented in Table 3. The AUROC values of PDFF for differentiating between grade S0 vs. S1–3, S0–1 vs. S2–3, and S1–2 vs. S3 were

0.922 (95% CI 0.889–0.956), 0.924 (95% CI 0.876–0.973), and 0.958 (95% CI 0.917–0.998), respectively. Corresponding values of CAP were 0.806 (95% CI 0.750–0.863), 0.795 (95% CI 0.719–0.871), and 0.760 (95% CI 0.538–0.981), respectively.

**Comparison of diagnostic accuracies for staging liver steatosis between PDFF and CAP**

PDFF showed significantly greater AUROCs than CAP in predicting S1–3 (0.922 vs. 0.806,  $P < 0.001$ , post hoc statistical power = 0.96) and S2–3 (0.924 vs. 0.795,  $P = 0.005$ , post hoc statistical power = 0.94). In fivefold cross-validation analysis, the AUROC value of PDFF was greater than that of

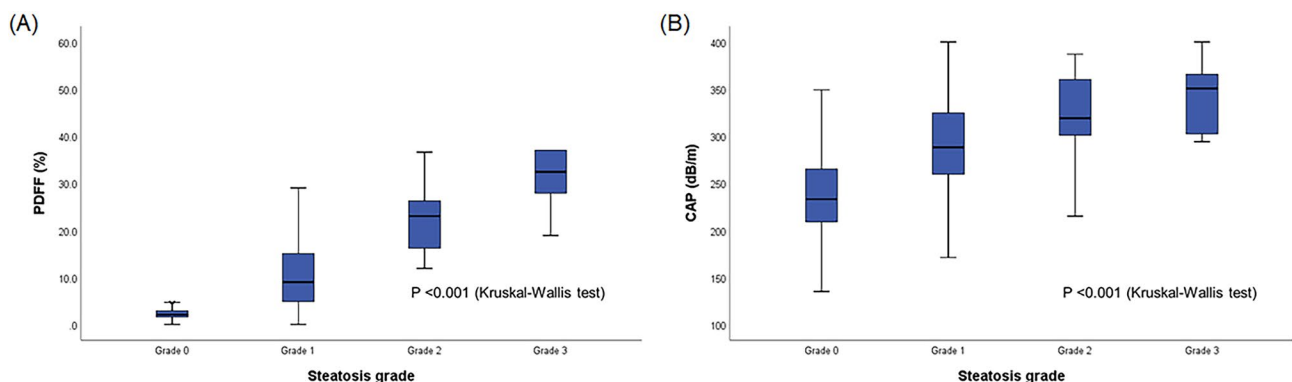


**Fig. 5** Liver steatosis value measured by PDFF (A) and CAP (B) according to each steatosis grade (S0–3). The horizontal line through each box represents the median and each box represents data from the

25th to the 75th percentile. The separate asterisks and circles represent outliers. *PDFF* proton density fat fraction, *CAP* controlled attenuation parameter

CAP for detecting S1–3 (0.852 vs. 0.760) and S2–3 (0.906 vs. 0.840). For the detection of S3 steatosis as compared with S0–2, PDFF and CAP had similar AUROC values (0.958 vs. 0.760,  $P=0.086$ ) (Fig. 6).

### Cutoff values of PDFF and CAP for staging liver steatosis

We evaluated the potential cutoff values of PDFF and CAP for the detection of each liver steatosis grade. The cutoff values of PDFF for differentiating between grade S0 vs. S1–3, S0–1 vs. S2–3, and S0–2 vs. S3 were 4.2%, 11.9%, and 18.9%, respectively. The corresponding values of CAP were 256, 294, and 298 dB/m, respectively.

Using a cutoff value of 4.2%, PDFF had a sensitivity of 85.7%, specificity of 87.6%, PPV of 93.2%, and NPV of 75.7% for detecting mild steatosis (S1–3). A CAP value of 256 dB/m predicted a mild steatosis with a sensitivity of 82.0%, specificity of 69.7%, PPV of 83.0%, and NPV of 68.1%.

For the prediction of S2–3 steatosis, PDFF had a sensitivity of 97.7%, specificity of 76.8%, PPV of 45.7%, and NPV of 99.4% with a cutoff value of 11.9%. Using a cutoff value of 294 dB/m, CAP showed a sensitivity of 84.2%, specificity of 71.2%, PPV of 34.4%, and NPV of 96.2% for detecting moderate steatosis. The representative images of MRE and TE are presented in Fig. 7.

### Discussion

In this study, we compared the diagnostic accuracy of TE and MRE for determining the degree of liver fibrosis and CAP and PDFF for assessing liver steatosis. We found positive correlations between both  $LS_{MRE}$  and  $LS_{TE}$  and the degree of histologically confirmed liver fibrosis. Positive correlation was also found between CAP and PDFF and

the degree of histologically confirmed liver steatosis. We also found that  $LS_{MRE}$  was significantly more accurate than  $LS_{TE}$  in identifying subjects with significant fibrosis (F2–4), whereas  $LS_{MRE}$  and  $LS_{TE}$  similarly predicted advanced fibrosis (F3–4) and cirrhosis (F4). In addition, PDFF had a significantly greater diagnostic accuracy than CAP in predicting mild (S1–3) or moderate steatosis (S2–3), whereas both had similar diagnostic accuracy in predicting severe steatosis (S3).

Our study has several clinical implications. First, liver fibrosis is the single most important factor that determines the outcome of patients with CLD. Therefore, early detection and assessment of the severity of liver fibrosis are crucial, because early medical intervention to improve liver fibrosis could yield better clinical outcomes [27–29]. In our study, we found a stepwise increase in  $LS_{MRE}$  and  $LS_{TE}$  in association with the degree of liver fibrosis (all  $P < 0.001$ ), in agreement with those of previous studies [18, 30, 31]. The increase in LS occurs in small increments during the early stages of fibrosis (F0–2), but in larger increments in advanced stages of fibrosis (F3–4), which might help MRE and TE accurately identify more advanced stages of fibrosis. Moreover, the diagnostic accuracy, reflected by AUROC, showed a trend to increase in association with the increase in histologic fibrosis grade.

Second, the diagnosis of early compensated liver cirrhosis is clinically important, because the risk of HCC development and decompensation abruptly increases in these patients [32]. In addition, early diagnosis of significant liver fibrosis is of paramount importance, because early medical intervention might help delay the progression of fibrosis to liver cirrhosis or even a higher chance of fibrosis regression, resulting in favorable long-term outcomes [21, 33]. In our study,  $LS_{MRE}$  had a significantly greater diagnostic accuracy than  $LS_{TE}$  in detecting significant liver fibrosis (F2–F4) (AUROC 0.846 vs. 0.781,  $P=0.046$ ). Using a cutoff value

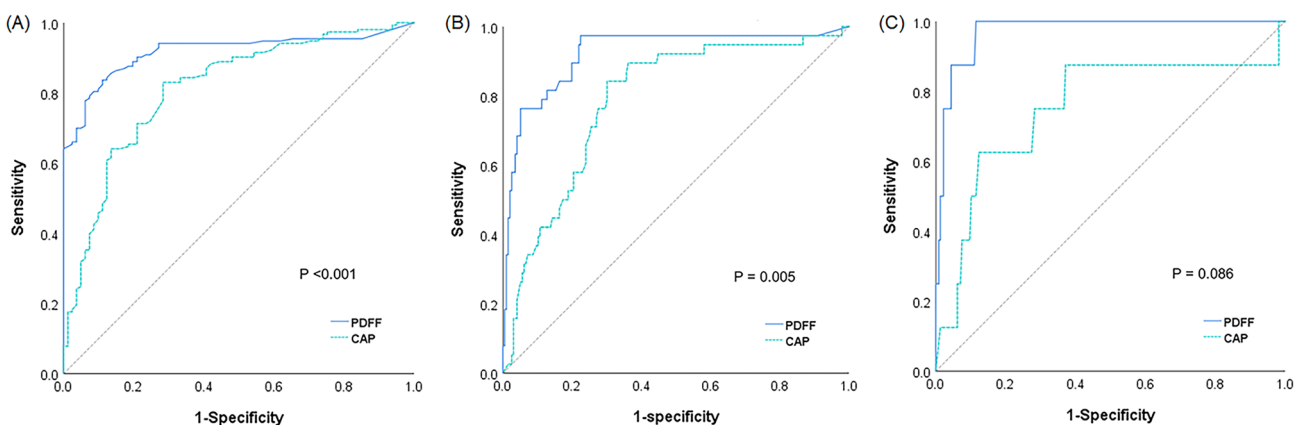


**Fig. 6** The area under the receiver operating characteristic curve of PDFF and CAP values for staging liver steatosis; S1–3 (A), S2–3 (B), and S3 (C). PDFF proton density fat fraction, CAP controlled attenuation parameter

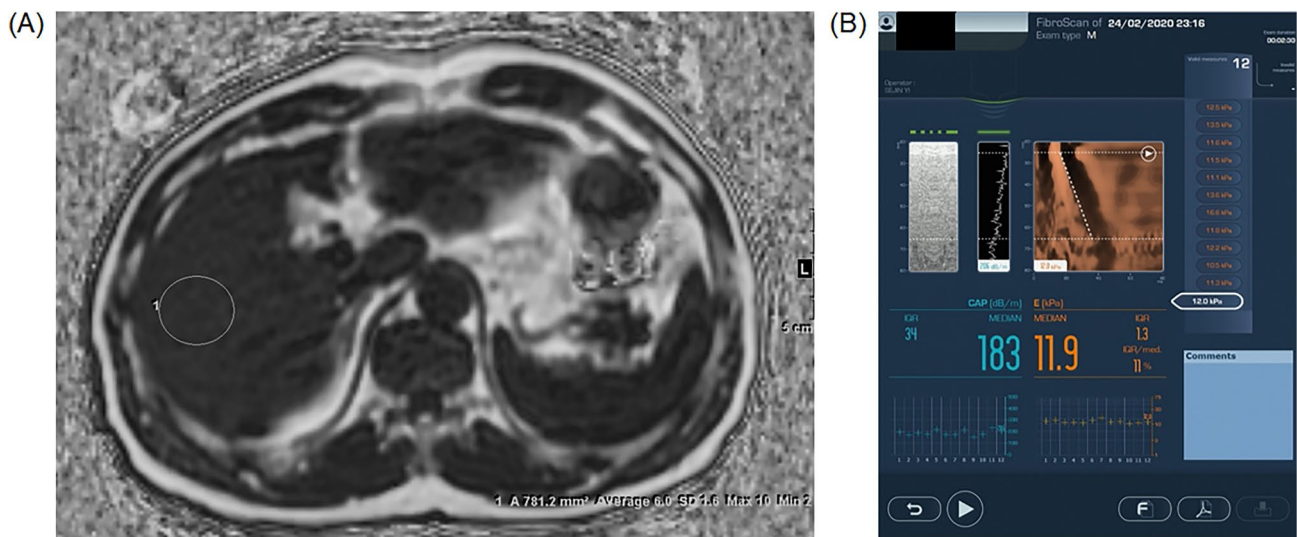


**Fig. 7** A 63-year-old male patient with newly diagnosed hepatocellular carcinoma underwent magnetic resonance PDFF and CAP. **A** Representative image of PDFF measurement is shown with the oval ROI drawn on the right posterior section of the liver. The area and the mean fat fraction of the ROI are 7.8 cm<sup>2</sup> and 6.0%, respectively. Final liver fat fraction was 5.6%, which was calculated by averaging the total of four ROI measurements. Liver steatosis grade of S1–3

was suggested, using a cutoff value of 4.2%. **B** Summary of TE measurement is shown with the CAP value of 183 dB/m, which suggests liver steatosis grade of S0 based on a cutoff value of 256 dB/m. Liver resection was performed, and the histopathologic grade of liver steatosis was S1 with a 10% of hepatocytes containing macrovesicular fat. PDFF proton density fat fraction, TE transient elastography, CAP controlled attenuation parameter, ROI region of interest

of 3.1 kPa, MRE had a sensitivity of 71.8% and a specificity of 84.8%. This finding might indicate that MRE might overcome the well-known unsatisfactory diagnostic accuracy of TE in identifying subjects with significant liver fibrosis. However, it should be further investigated who can benefit from MRE assessment in diagnosing fibrotic burden and predicting long-term outcomes during the course of liver disease, because of the high cost and low accessibility of MR devices.

Third, in our study, steatosis was not associated with  $LS_{MRE}$  or  $LS_{TE}$  (all  $P > 0.05$ ). In accordance with our results, a recent study with CHB patients demonstrated no significant difference in LS value obtained with TE according to the severity of hepatic steatosis among patients with F2–F4 fibrosis [34]. In addition, a recent study reported the negligible effect of liver steatosis on the cutoff value of LS measured using MRE to discriminate significant liver fibrosis [30].

Fourth, hepatic fat accumulation is receiving increasing attention, because the prevalence of fatty liver disease and concurrent liver steatosis in other CLDs is dramatically affecting developed countries. In our study, a significant stepwise association between PDFF and CAP value and histologic degree of liver steatosis was found (all  $P < 0.001$ ). PDFF had a significantly higher diagnostic accuracy than CAP in predicting S1–3 (AUROC 0.922 vs. 0.806,  $P < 0.001$ ) and S2–3 (AUROC 0.924 vs. 0.795,  $P = 0.005$ ) steatosis. To date, two studies have demonstrated

the superior diagnostic accuracy of PDFF to that of CAP in assessing the degree of histologic liver steatosis in patients with NAFLD. One study showed a significantly higher diagnostic accuracy of PDFF than CAP in diagnosing all stages of liver steatosis [18]. In contrast, the other demonstrated an inferior diagnostic accuracy of CAP compared to that of PDFF in detecting S2–3 and S3 steatosis [35]. Although some controversy still remains, based on previous studies and ours, the diagnosis of liver steatosis using PDFF might be more accurate than, or at least similar to, that of CAP.

Lastly, we included patients with different etiologies, to compare the diagnostic accuracy of TE and MRE in various etiologies of CLD patients. Most studies have evaluated patients with single etiology, such as NAFLD [18–20, 30], metabolic-associated fatty liver disease [35], or alcoholic liver disease [31].

Despite several strengths, we are also aware of the pitfalls in our study, which remain unresolved. First, we used histopathological information as the gold standard; however, it is also subjected to intra- and inter-observer variability and sampling errors. Second, selection bias may be present, because of the retrospective design of the study with a biased selection of subjects with MR assessment. Third, the AUROCs and cutoff values of  $LS_{MRE}$  for detecting F2–4 and F3–4 were lower than those reported in previous studies [17–20]. We assume that the relatively small number of patients, especially in subgroups of advanced fibrosis might affect the diagnostic accuracy of MRE, representing lower

AUROC and cutoff values. In addition, small number of patients in subgroups of moderate and severe liver steatosis might limit the accurate evaluation of the diagnostic accuracy of PDFF and CAP. Fourth, although recent studies show the predictive value of MRE in outcome of CLD patients, we could not analyze that because of the short follow-up period; however, those have no histologic results [36, 37]. Lastly, although the drawing of ROIs on the MR images is not yet fully standardized, we tried to minimize the potential bias by measuring three or four ROIs.

In conclusion, MRI exhibited significantly higher diagnostic accuracy than TE for detecting significant fibrosis and mild or moderate steatosis in patients with CLD. However, the limited availability of MR devices in specific areas should be resolved for the widespread use of MRI-based assessment for liver fibrosis and steatosis.

**Acknowledgements** We would like to thank Editage ([www.editage.co.kr](http://www.editage.co.kr)) for English language editing.

**Author contributions** JC, BJP, and SUK: Conception and design, JC, BJP, and SUK: Development of methodology, HAL, SK, and YSS: Acquisition, analysis, and interpretation of data, HAL, SK, and YSS: Writing, reviewing, and/or revision of the manuscript, SUK: Administrative, technical, or material support, JC, BJP, and SUK: Study supervision.

**Funding** None.

## Declarations

**Conflict of interest** Seung Up Kim has served as an advisory committee member Gilead Sciences, GSK, Bayer, and Eisai. He is a speaker for Gilead Sciences, GSK, Bayer, Eisai, Abbvie, EchoSens, MSD, and Bristol-Myers Squibb. He has also received a research grant from Abbvie and Bristol-Myers Squibb. The other authors declare that they have no competing interests.

**Ethical approval** The study protocol was in accordance with the ethical guidelines of the 1975 Declaration of Helsinki and was approved by the human ethics committee of each hospital (Institutional Review Board of Korea University College of Medicine, Yonsei University College of Medicine).

**Informed consent** The requirement for informed consent was waived because of the retrospective design of the study.

## References

1. Younossi ZM, Stepanova M, Rafiq N, Makhlof H, Younoszai Z, Agrawal R, Goodman Z. Pathologic criteria for nonalcoholic steatohepatitis: interprotocol agreement and ability to predict liver-related mortality. *Hepatology* 2011;53:1874-1882.
2. Yano M, Kumada H, Kage M, Ikeda K, Shimamatsu K, Inoue O, Hashimoto E, et al. The long-term pathological evolution of chronic hepatitis C. *Hepatology* 1996;23:1334-1340.
3. Ekstedt M, Hagström H, Nasr P, Fredrikson M, Stål P, Kechagias S, Hultcrantz R. Fibrosis stage is the strongest predictor for disease-specific mortality in NAFLD after up to 33 years of follow-up. *Hepatology* 2015;61:1547-1554.
4. Lee YB, Ha Y, Chon YE, Kim MN, Lee JH, Park H, Kim KI, et al. Association between hepatic steatosis and the development of hepatocellular carcinoma in patients with chronic hepatitis B. *Clin Mol Hepatol* 2019;25:52-64.
5. EASL-ALEH Clinical Practice Guidelines: Non-invasive tests for evaluation of liver disease severity and prognosis. *J Hepatol* 2015;63:237-264.
6. Intraobserver and interobserver variations in liver biopsy interpretation in patients with chronic hepatitis C. The French METAVIR Cooperative Study Group. *Hepatology* 1994;20:15-20.
7. Kleiner DE, Brunt EM, Van Natta M, Behling C, Sanyal AJ, et al. Nonalcoholic Steatohepatitis Clinical Research Network. Design and validation of a histological scoring system for nonalcoholic fatty liver disease. *Hepatology*. 2005 Jun;41(6):1313-21.
8. Bedossa P, Dargère D, Paradis V. Sampling variability of liver fibrosis in chronic hepatitis C. *Hepatology* 2003;38:1449-1457.
9. Rousselet MC, Michalak S, Dupré F, Croué A, Bedossa P, Saint-André JP, Calès P. Sources of variability in histological scoring of chronic viral hepatitis. *Hepatology* 2005;41:257-264.
10. Piccinino F, Sagnelli E, Pasquale G, Giusti G. Complications following percutaneous liver biopsy. A multicentre retrospective study on 68,276 biopsies. *J Hepatol* 1986;2:165-173.
11. Zhang X, Wong GL, Wong VW. Application of transient elastography in nonalcoholic fatty liver disease. *Clin Mol Hepatol* 2020;26:128-141.
12. Kjærsgaard M, Thiele M, Jansen C, Stæhr Madsen B, Gørtzen J, Strassburg C, Trebicka J, et al. High risk of misinterpreting liver and spleen stiffness using 2D shear-wave and transient elastography after a moderate or high calorie meal. *PLoS One* 2017;12:e0173992.
13. Ratchataseetakul K, Rattanasiri S, Promson K, Sringam P, Sobhonslidsuk A. The inverse effect of meal intake on controlled attenuation parameter and liver stiffness as assessed by transient elastography. *BMC Gastroenterol* 2017;17:50.
14. Vuppalanchi R, Weber R, Russell S, Gawrieh S, Samala N, Slaven JE, Harden L, et al. Is Fasting Necessary for Individuals With Nonalcoholic Fatty Liver Disease to Undergo Vibration-Controlled Transient Elastography? *Am J Gastroenterol* 2019;114:995-997.
15. Wong VW, Lampertico P, de Lédinghen V, Chang PE, Kim SU, Chen Y, Chan HL, et al. Probability-based interpretation of liver stiffness measurement in untreated chronic hepatitis B patients. *Dig Dis Sci* 2015;60:1448-1456.
16. Wong GL, Wong VW, Choi PC, Chan AW, Chim AM, Yiu KK, Chan FK, et al. Increased liver stiffness measurement by transient elastography in severe acute exacerbation of chronic hepatitis B. *J Gastroenterol Hepatol* 2009;24:1002-1007.
17. Singh S, Venkatesh SK, Wang Z, Miller FH, Motosugi U, Low RN, Hassanein T, et al. Diagnostic performance of magnetic resonance elastography liver fibrosis: a systematic review and meta-analysis of individual participant data. *Clin Gastroenterol Hepatol* 2015;13:440-451.e446.
18. Imajo K, Kessoku T, Honda Y, Tomeno W, Ogawa Y, Mawatari H, Fujita K, et al. Magnetic Resonance Imaging More Accurately Classifies Steatosis and Fibrosis in Patients With Nonalcoholic Fatty Liver Disease Than Transient Elastography. *Gastroenterology* 2016;150:626-637.e627.
19. Furlan A, Tublin ME, Yu L, Chopra KB, Lippello A, Behari J. Comparison of 2D Shear Wave Elastography, Transient Elastography, and MR Elastography for the Diagnosis of Fibrosis in Patients With Nonalcoholic Fatty Liver Disease. *AJR Am J Roentgenol* 2020;214:W20-w26.
20. Park CC, Nguyen P, Hernandez C, Bettencourt R, Ramirez K, Fortney L, Hooker J, et al. Magnetic Resonance Elastography vs

- Transient Elastography in Detection of Fibrosis and Noninvasive Measurement of Steatosis in Patients With Biopsy-Proven Nonalcoholic Fatty Liver Disease. *Gastroenterology* 2017;152:598-607. e592.
21. Kang SH, Lee HW, Yoo JJ, Cho Y, Kim SU, Lee TH, Jang BK, et al. KASL clinical practice guidelines: Management of nonalcoholic fatty liver disease. *Clin Mol Hepatol* 2021;27:363-401.
  22. Soon G, Wee A. Updates in the quantitative assessment of liver fibrosis for nonalcoholic fatty liver disease: Histological perspective. *Clin Mol Hepatol* 2021;27:44-57.
  23. Guglielmo FF, Venkatesh SK, Mitchell DG. Liver MR Elastography Technique and Image Interpretation: Pearls and Pitfalls. *Radiographics* 2019;39:1983-2002.
  24. Sofue K, Mileto A, Dale BM, Zhong X, Bashir MR. Interexamination repeatability and spatial heterogeneity of liver iron and fat quantification using MRI-based multistep adaptive fitting algorithm. *J Magn Reson Imaging* 2015;42:1281-1290.
  25. Jung KS, Kim SU. Clinical applications of transient elastography. *Clin Mol Hepatol* 2012;18:163-173.
  26. DeLong ER, DeLong DM, Clarke-Pearson DL. Comparing the areas under two or more correlated receiver operating characteristic curves: a nonparametric approach. *Biometrics* 1988;44:837-845.
  27. Martinez SM, Foucher J, Combis JM, Métivier S, Brunetto M, Capron D, Bourlière M, et al. Longitudinal liver stiffness assessment in patients with chronic hepatitis C undergoing antiviral therapy. *PLoS One* 2012;7:e47715.
  28. Marcellin P, Gane E, Buti M, Afdhal N, Sievert W, Jacobson IM, Washington MK, et al. Regression of cirrhosis during treatment with tenofovir disoproxil fumarate for chronic hepatitis B: a 5-year open-label follow-up study. *Lancet* 2013;381:468-475.
  29. Campana L, Iredale JP. Regression of Liver Fibrosis. *Semin Liver Dis* 2017;37:1-10.
  30. Chen J, Allen AM, Therneau TM, Chen J, Li J, Hoodeshenas S, Chen J, Lu X, Zhu Z, Venkatesh SK, Song B, Ehman RL, Yin M. Liver stiffness measurement by magnetic resonance elastography is not affected by hepatic steatosis. *Eur Radiol.* 2022 Feb;32(2):950-958.
  31. Bensamoun SF, Leclerc GE, Debernard L, Cheng X, Robert L, Charleux F, Rhein C, et al. Cutoff values for alcoholic liver fibrosis using magnetic resonance elastography technique. *Alcohol Clin Exp Res* 2013;37:811-817.
  32. KASL clinical practice guidelines for liver cirrhosis: Varices, hepatic encephalopathy, and related complications. *Clin Mol Hepatol* 2020;26:83-127.
  33. KASL clinical practice guidelines for management of chronic hepatitis B. *Clin Mol Hepatol* 2019;25:93-159.
  34. Shen F, Mi YQ, Xu L, Liu YG, Wang XY, Pan Q, Zhang RN, et al. Moderate to severe hepatic steatosis leads to overestimation of liver stiffness measurement in chronic hepatitis B patients without significant fibrosis. *Aliment Pharmacol Ther* 2019;50:93-102.
  35. Shao CX, Ye J, Dong Z, Li F, Lin Y, Liao B, Feng S, et al. Steatosis grading consistency between controlled attenuation parameter and MRI-PDFF in monitoring metabolic associated fatty liver disease. *Ther Adv Chronic Dis* 2021;12:20406223211033119.
  36. Gidener T, Yin M, Dierkhising RA, Allen AM, Ehman RL, Venkatesh SK. Magnetic resonance elastography for prediction of long-term progression and outcome in chronic liver disease: A retrospective study. *Hepatology.* 2022 Feb;75(2):379-390.
  37. Gidener T, Ahmed OT, Larson JJ, Mara KC, Therneau TM, Venkatesh SK, Ehman RL, Yin M, Allen AM. Liver Stiffness by Magnetic Resonance Elastography Predicts Future Cirrhosis, Decompensation, and Death in NAFLD. *Clin Gastroenterol Hepatol.* 2021 Sep;19(9):1915-1924.e6.

**Publisher's Note** Springer Nature remains neutral with regard to jurisdictional claims in published maps and institutional affiliations.

Springer Nature or its licensor holds exclusive rights to this article under a publishing agreement with the author(s) or other rightsholder(s); author self-archiving of the accepted manuscript version of this article is solely governed by the terms of such publishing agreement and applicable law.